The fictional transition of the preferential orientation of Yttria-stabilized Zirconia thin films

J. S. Lamas[a,1*], W.P. Leroy[a,] and D. Depla[a]

[a] Research Group DRAFT, Department of Solid State Sciences, Ghent University, Krijgslaan 281/S1 9000 Ghent, Belgium

[*]Corresponding author. Tel.: +32-9-264-4368; Fax: +32-9-264-4996

E-mail: Jerika.Lamas@UGent.be

Abstract

The fundamental study of the microstructural and textural evolution of Yttria-Stabilized Zirconia (YSZ) thin films is of great importance as the crystallographic properties are intimately related to their extrinsic or functional properties. In order to study these properties, YSZ thin films were obtained using dual magnetron sputtering. The results of a polar plot graph, based on X-ray diffraction (XRD) data, seems to indicate a transition from [200] out-of-plane preferential orientation to [111], being dependent on composition and yttrium target-substrate (Y T-S) distance at low pressure. However, no transition is identified at high pressure, showing only [111] out-of-plane orientation, independent on composition and Y T-S distance. Scanning electron microscopy (SEM) shows a tilt in the columnar structure of the film but no other microstructural change is noticed which could be related to the growth transition from [200] to [111]. Pole figures were used to clarify the texture transition in the YSZ thin films. These results indicate that there is indeed no transition in the preferential orientation of the films from [200] to

[111] but a tilt of the [200] direction towards the zirconium source. The detailed study using pole figures and SEM, clearly shows that, in contradiction to what standard theta/2theta XRD measurements hint, no growth zone transition is present and the effect is caused by the geometrical configuration.

Keywords: YSZ thin films; magnetron sputtering; preferential orientation; flux of metal particles; energy per deposited atom.

1. Introduction

Complex oxide materials play an important role in different application fields. Characteristics such as high ionic conductivity, low electrical conductivity and high mechanical properties [1,2] make them interesting materials. Yttria-Stabilized Zirconia (YSZ), e. g. has been extensively studied for many applications [3,4] but especially as an electrolyte for oxygen sensors[5] and in Solid Oxide Fuel Cells (SOFC) [6-12]. Although SOFC have a high efficiency, their operation is limited by the ionic conductivity of the electrolyte which depends on the working temperature (700 – 1000°C). A possible solution to decrease this operating temperature is to reduce the thickness of the YSZ electrolyte. A vast amount of literature data on these materials is present, but mostly related to bulk YSZ and thick films [12-14]. However, downscaling it to a thin film changes the fundamental aspects of the oxygen ion conduction due to the occurrence of small scale or nano effects. That is why a good understanding of the fundamental aspects of their growth would open the possibility to manipulate the ionic conductivity by controlling the microstructure and texture of the thin film.

In this study, YSZ thin films were deposited by dual reactive magnetron sputtering [15,16,17], a so-called physical vapor deposition (PVD) technique. This technique allows to deposit thin films ranging in thickness from a few nanometers to micrometers and to investigate the compositional influence in a flexible way. The composition of the deposited thin film can influence the fundamental processes occurring during the growth of the thin film. Therefore, it is immensely important to study the relationship between the deposition conditions, microstructure and texture. This relationship has been investigated before [18] for TiN, MgO, YSZ and Cr systems. In our previous work [19], the thin film morphology (and texture) of YSZ as a function of both composition and target-substrate (T–S) distance was studied. The preferential orientation was determined based on the competition between the fastest growth direction and the lowest surface energy. However, some unresolved trends remained involving the effects of composition and the deposition geometry on the growth of YSZ thin films.

This paper first discusses the influence of target-substrate (T-S) distance and composition on the crystallographic properties of YSZ thin films deposited at two different gas pressures. A correlation is deduced describing the preferential crystallographic orientation behavior when either T-S distance or composition is changed. Determination of the energy per deposited atom provides more information on the effect of energy on the film growth mechanism. Secondly, scanning electron microscopy (SEM) images are presented to discuss the film growth in terms of the extended structure zone model (ESZM) [18]. Furthermore, pole figures were obtained in order to clarify the transition of the preferential orientation of YSZ thin films as well to correlate it to the information obtained with the former analysis. Finally, measurements with different substrate angles were performed to corroborate the conclusions obtained in this work.

2. Experimental setup

Reactive unbalanced magnetron sputtering was used to deposit YSZ thin films. All thin films were deposited on amorphous glass substrates (76 mm x 22 mm) in a stainless steel vacuum chamber. This chamber was pumped via a combination of a turbo-molecular and a rotary pump, reaching a base pressure of 10^{-4} Pa. Two magnetrons were positioned 45° to the substrate holder and metallic Y and Zr targets were mounted, respectively. The substrate holder was grounded and was neither heated nor cooled during the deposition. The oxygen flow was oriented directly to the substrate, maximizing film oxidation and avoiding target poisoning. Prior to the beginning of the deposition, experimental conditions were stabilized by protecting the substrate with a shutter. The magnetrons are powered using a DC power supply (Hüttinger Elektronik), working in constant current mode (I_Y = 0.2 A, I_{Zr} = 0.5 A). The Y target-substrate (T-S) distance was changed at different gas pressures (0.5 Pa and 0.95 Pa). The deposition time was equal to 20 minutes. All YSZ coatings were transparent, fully oxidized in the cubic phase and presented biaxial alignment, i.e., there is not only a preferential out-of-plane orientation, but also an in-plane orientation of the constituent crystallites. Further experimental details can be found in Lamas et al.[19].

The film composition was measured using energy-dispersive X-ray spectroscopy analysis (EDX) and micrographs were obtained via scanning electron microscope (SEM). X-ray diffraction (XRD) in theta-2theta configuration was performed on all samples and the data was converted to a polar plot graph. Pole figure measurements, using a Sol-X energy dispersive detector, were used to evaluate the crystallinity and the biaxial alignment of the YSZ thin films. In these pole

figures, χ (polar angle) was varied from 0-80° and φ (azimuthal angle) from 0-360°, in steps of 5°.

The determination of the energy flux was performed using a passive thermal probe [20]. The thermal probe was positioned in the center of the sample holder. The experimental conditions remained the same as mentioned above.

3. Results and Discussion

3.1 Influence of pressure on the preferential orientation of YSZ thin films

YSZ thin films were deposited at two different gas pressures: 0.5 and 0.95 Pa. The composition along the film was controlled by changing the Y T-S distance from 80 to 240 mm in steps of 20 mm. Other parameters such as discharge currents, Zr T-S distance (90 mm) and deposition time remained constant. The O_2 flow varied from 1.2 to 3 sccm depending on the target erosion and on the gas pressure. Moreover, the highest deposition rate was assured to completely oxidize the films in the metallic mode. Film thicknesses were encountered between 0.5 to 1 µm depending on the Y T-S distance and composition.

In our previous work, the out-of-plane preferential orientation of these films was shown in a polar plot graph [19]. The orientation of a crystal with known unit cell dimensions can be represented in this plot. The main advantage of this representation is that influences generated by the proximity of certain cubic crystal directions or a possible rotation of the crystal are easily detected. Furthermore, the preferential orientation of the film can easily be appointed.

For each sample, a resultant vector was calculated using stereographic projections of the [111], [200] and [220] fractions. The resultant vector will have a resultant point in the triangular plane formed by these directions. The resultant vector is formed by two angle components, namely a polar (χ: 0-90°) and an azimuthal (φ: 0-360°) angle. For example, a single crystalline [200] sample would have its resultant vector with $\chi = 90°$ and $\varphi = 0°$.

Fig. 1 shows the polar plot of the films deposited at different pressures. The color scale represents the content of Y in the film. At low pressure (p = 0.5 Pa), the graph indicates that [200] is the preferential orientation for low contents of Y and/or high T-S distance. A transition from [200] to [111] occurs when the Y content increases. A gap towards the [220] direction can be seen ($\chi = 60°$ and $\varphi = 30°$), representing the contribution of this latter direction in the XRD pattern. For very high Y content the film reaches the [111] direction. At higher pressure (p = 0.95 Pa), however, there is no evident transition from [200] to [111]. The points remain very close to the [111] region. It can be assumed, then, that at high pressure there is no dependence on Y content and/or T-S distance.

3.2 Influence of pressure and distance on the energy flux towards the YSZ film

To pinpoint the growth model for the YSZ films (next sections), the thermal flux towards the growing film is examined at different growth conditions. Fig. 2 shows the variation of thermal flux, the flux of metal particles and the energy per deposited atom vs. Y T-S distance at different gas pressures. In Fig.2a, a decrease of the thermal flux is observed when Y T-S reaches approximately 140 mm, remaining constant within the error of the measurement. Therefore, there is only a minor influence of the pressure, and of the distance. This can be explained by the

position of the magnetrons. As one source (zirconium) is close to the substrate (90 mm), the effect of the other source (yttrium) is only minor, except for almost equal distances where there is a small increase of the energy flux. The reason for the small increase is due to the fact that the power of the nearest source has a value between 125 W (0.95 Pa) and 150 W (0.5 Pa), while the power of the moving source has a value between 45 W (0.95 Pa) and 55 W (0.5 Pa), eliminating the inverse square effect of the distance [21].

An interpretation of the thermal flux was then considered on basis of the energy per deposited atom. This energy consists of the measured thermal flux normalized by the flux of metal particles. Due to the gradient of composition and thickness in the samples, the flux of metal particles is defined considering the specific mass and thickness of the film [22]. The flux of metal particles is then given by equation (1)

$$F_M = \frac{R_d \times e \times N_A}{\left[\left(\frac{\%Y}{2} \times \frac{M_{Y2O3}}{\rho_{Y2O3}}\right) + \left(\%Zr \times \frac{M_{ZrO2}}{\rho_{ZrO2}}\right)\right]}, \qquad (1)$$

where e is the elementary charge, N_A is the Avogadro's constant, R_d is deposition rate (thickness of the sample related to a specific composition divided by deposition time), %Y and %Zr are the atomic percentage of metallic Y and Zr, respectively, M is the molar mass and ρ is the density of both oxides.

The flux of metal particles is not only related to the Y T-S distance but also to the gas pressure. In Fig. 2b both influences are shown. With the change of Y T-S distance to higher values, there is a reduction of the flux of metal particles because of the small solid angle and the increase of the gas scattering. The effect of the pressure is mainly due to the lowering of the discharge voltage at higher pressures [23-26], reducing the sputter yield of the target material.

Two hypotheses can be proposed to explain the textural change of the thin films. One is based on the mobility of the arriving species defining the growth zone in the extended structure zone model. The mobility is defined by the total energy per deposited atom (EPA), which is the ratio between the thermal flux and the flux of metal particles. This relation provides more information on the possible effect of energy on the film growth mechanism. As demonstrated in Fig. 2c, the increase of the gas pressure from 0.5 to 0.95 Pa increases the total energy per deposited atom [27,28,29]. This effect can be understood from the almost constant energy flux and the lowering of the deposition rate. The ratio between the EPA at low pressure and high pressure is only 1.5. Moreover, the change within one pressure series is also quite small. Therefore, the noticed textural changes as shown in Figure 1 are hard to explain from a change in the EPA. Indeed, as shown before by our research group [30,31], a textural change could be explained by a transition from zone T to zone II growth. However, for this kind of transition to happen, the mobility, and therefore the EPA, must drastically increase. Typically, the EPA changes over an order of magnitude. The reason for this drastic increase is due to target poisoning, reducing the deposition rate substantially. In this study, target poisoning was prevented by the use of a local oxygen inlet, resulting in a minor change of the deposition rate (see Figure 2b).

Another hypothesis to explain the textural change of the thin film is based on previous work published by our group. It was shown that the nature of the adsorbing reactive gas species (atomic oxygen or molecular oxygen) also influences the textural evolution. At high concentrations of atomic oxygen in the plasma, YSZ thin films can grow [111], while a [200] out-of-plane orientation is noticed at low atomic oxygen concentration. In both cases, there is no microstructural change, i.e. the films grow with a zone T microstructure. However, by working in metallic mode, the concentration of oxygen in the plasma is very low [32]. Therefore, it can be

expected that also a change of the nature of the adsorbing reactive species from molecular to atomic cannot explain the noticed behavior.

3.3 Growth model of YSZ thin films

SEM images of the surface and cross section at low and high pressures can help to elucidate the growth behavior of the YSZ thin films. Fig. 3 represents the cross sections and a plan view of the YSZ at different conditions. The columnar structure is clearly observed in the cross sections. Furthermore, a tilt of the columns is noticed. Based on the analysis of several samples it is clear that the columns tilt towards the magnetron source which provides the metallic adparticle with the smallest ionic radius, Zr. The difference in the ionic radius (r_{Zr} = 0.72 Å; r_Y = 0.9 Å) together with the compositional gradient on the sample are, then, the cause of the columnar tilt during the film growth. A similar behavior was also observed for the AlInN [33] and Mg(M)O [34] system.

At low pressure (Fig.3a, b and c) the V-shaped facetted columns are clearly identified, and the pyramidal surface shape can be clearly seen in Fig. 3b. At high pressure however, a distorted V-shape is present. This distortion can be related with the mobility of adparticles and the flux of material arriving on the substrate since the energy per deposited atom is higher as shown in Fig. 2c. Furthermore for these conditions, a thicker columnar structure is observed in the film due to the higher amount of energy per adparticle delivered to the growing film and hence, an increased mobility of the adparticles.

In agreement with the discussion in section 3.2, the transition from zone T growth to zone II, which was hinted by the XRD polar plot analysis, is not recognized by the SEM analysis, excluding the hypothesis that the transition is due to the small increase of the EPA. As this

observation is completely contradictory to the general accepted behavior for the growth of thin films, more detailed results are discussed.

The following section, based on pole figure plots, will elucidate which preferential orientation is present in the films and hence how these films' growth fit in the ESZM.

3.4 Influence of the geometrical configuration on YSZ films

Standard theta/2theta XRD analysis (summarized in the polar plot results) indicate a transition in the preferential orientation from [200] to [111] with the increase of Y content and/or T-S distance at low pressure. In the SEM images however, this transition was not identified. To clarify the behavior of YSZ thin films and correlate it with the information obtained in prior analysis, XRD pole figures were measured.

Prior to this clarification, it is important to accentuate that the pole figure measurements confirm the results obtained via the polar plot. The calculated angle in χ and φ of the polar plot is equivalent to the main [200] peak in the pole figure and it can be easily identified when represented in a stereographic projection. An example for [200] peak at $\varphi = 12°$ and $\chi = 78°$ is demonstrated in Fig. 4.

Fig. 5 and 6 show pole figures with different Y T-S distances at low and high pressure, respectively. The first column indicates the [111] pole figure, followed in the middle by the [200] pole figure, and finally, the third column represents the schematic drawing of the cubic structure based on the angles obtained in the polar plot analysis.

The biaxial alignment for YSZ thin films can be observed in these images. At low pressure and low content of Y (or high T-S distance, Fig. 5a) the [200] is identified to be the out-of-plane

preferential orientation, with a clear peak in the center of the [200] figure (white ball on the schematic drawing). As the Y content increases (decrease of T-S distance) there is a tilt on the out-of-plane preferential orientation from [200] to [111].

The Y and Zr magnetrons are positioned on the left and right hand side of the plotted poles, respectively. It is noticeable that the tilt follows the metal with the smallest ionic radius, Zr, as it was indicated in the SEM images. Note that for very high contents of Y and small Y T-S distance (Fig. 5c), the YSZ film does not reach a pure [111] out-of-plane preferential orientation but it still presents a strong tilt in the [200] orientation. This is also identified in the polar plot by the arc towards [111]. This tilt allows other directions to be identified by the incident X-ray, because the XRD technique obtains the reflections of the various planes which interfere constructively to the Bragg peaks.

The schematic drawings of the lattice demonstrate this tilt and show how the cubic lattice should be positioned either in the [111] and [200] direction based on the pole figure.

Fig.6 shows the pole figures at higher pressure (p = 0.95 Pa), for different Y T-S distances. It is clear that at higher pressure the orientation is independent of the Y content and of the Y T-S distance, in agreement with the polar plot analysis.

The poles indicate a main [200] preferential orientation tilted in the direction of Zr (right hand side of the pole figure). The [111] peaks are located very close to the center of the pole and also two less intense peaks on the right side of the pole, indicating that the cubic structure is tilted as can be seen in the schematic drawing. The tilt is mainly constant for these samples and the variation seen in the polar plot in the region of $\chi = 70°$ and $\varphi = 35°$ can be attributed to the position of the substrate on the sample holder during deposition and also to the spot region measured in the pole figure measurements.

At high Y content (above 40% Y) the film loses its biaxial alignment becoming uniaxial aligned. This loss can be related to the mobility of the adparticles and also to the angular spread of the incoming material [18]. At higher pressure the arrival angle of the adparticles is strongly influenced by the collisions with the gas atoms, changing their direction towards the film surface, resulting in a less defined directed flux of the arriving atoms. In Fig. 6c, it is observed that the out-of-plane preferential orientation remains [200] and in the [111] direction, a semicircular shape is formed. This semicircular shape represents the contribution of all cubic [111], oriented in different directions.

Based on the pole figures it can first be concluded that the difference in the pole figures at low and high pressure is associated to the angular spread of the incoming material and also to the mobility of the adparticles, being more evident at higher contents of Y. Secondly, it was determined that the transition from [200] to [111] shown in the polar plot (and hence in standard theta/2theta) is in reality a tilt of the [200] in the direction of Zr target and not a transition between growth zones. This tilt was related to the geometrical configuration of the magnetrons, i.e. the position of the metal with the smallest ionic radius, determining the direction of the tilt. And finally, it was shown that the polar plot which is based on theta/2theta measurements can be interpreted in two ways: as the contribution of the fraction of the different oriented crystals and as the result of the tilting of the crystals. The pole figures represent the orientation distribution of the crystallographic planes, being a necessity to distinguish between the two interpretations of the polar plot.

In order to further prove that the tilt follows the smallest ionic radius, the substrate angle was changed towards the Y target and also to the Zr target and the results are displayed in the next section.

3.5 Changing substrate angle

As verified above, the geometrical configuration of the magnetrons and substrate are of fundamental importance for the growth of YSZ thin films. In order to evaluate the tilt behavior in YSZ thin films, measurements with different substrate angles were performed based on the geometrical factor, i.e., the configuration of magnetrons and substrate in the chamber.

The experiments follow the procedures explained in section 2. However, the measurements were only performed at low pressure. The inclinations of the substrate were +7.4° and -7.4°, where the positive sign indicates a tilt towards the Y target while the negative indicates a tilt towards the Zr target. The 0° tilt refers to the data discussed in section 3.1.

Fig 7 illustrates the plot of the azimuthal and polar angle vs. composition (content of Y in the film) based on the polar plot analyses. As a first approximation it is expected that the behavior of the transition remains the same, i. e. there is a tilt of the columns and consequently a tilt of the [200], indicating that the change of the substrate angle does not influence the columnar tilt. However, when the substrate angle is changed, the position of the Y and Zr target are different from the initial one (when substrate angle = 0°). This leads to different starting angles as can be seen at low composition in Fig. 7a and b. Although we do see a change in the curve slope at low composition when the substrate angle is different, the mechanism that leads to these different angles is still unclear. These data were analyzed by statistic t-tests demonstrating to be significant at low pressures. At approximately 25 at.% Y, there is a change of the slope of the curve and no significant difference is further noticed among the angles.

In short, it was determined that the change of tilt is related to geometrical factor since the growing of the [200] and its direction in the lattice was dependent on the substrate angle. A change of the substrate angle might change the starting angle of the tilt but does not change the columnar behavior of the tilted growing film. This behavior is yet unclear, and more work will help in unraveling this behavior.

4. Conclusion

Based on the XRD/polar plot analyses, a transition was determined in the out-of-plane preferential orientation from [200] to [111] in the biaxially aligned YSZ thin films, indicating a transition from growth zone T to growth zone II. The SEM images, however, did not identify such a transition, and therefore the use of pole figure plots was required to elucidate the change in the preferential orientation of YSZ thin films.

Determinations of the flux of metal particles and the energy per deposited atom were performed and corroborated the conclusion that no growth zone transition was present, in contradiction to what standard theta/2 theta XRD measurements hinted.

The results attest that the geometrical configuration of the deposition setup plays an important role on the preferential orientation of the thin film. This was indicated by the tilting of the [200] preferential out-of-plane direction towards the metal with the smallest ionic radius, which in this work corresponds to the Zr target. This tilt is dependent on the flux of metal particles arriving on the substrate. This flux was related to the Y content in the film and to the Y T-S distance at low pressure, but resulted to be independent when deposited at high pressure. Moreover, there was no change in the tilt at high pressure, and at high Y content the film losses its biaxial alignment

becoming uniaxially aligned. The change of the substrate angle suggested that the columnar tilt is not affected. However, it leads to different starting angles of the tilt at low Y composition. This mechanism is not yet clear.

In the presence of a tilt of the cubic lattice, the XRD identifies other directions which do not represent the real out-of-plane preferential orientation. It is important when working with a dual magnetron sputtering, to be aware of this when conclusions are made based on the XRD,, in order to avoid misleading information. As presented in this work, polar plot analysis and pole figures can be a very accurate technique to identify the preferential orientation of thin film and its behavior. However, it was shown that the polar plot can be interpreted in two different ways and that pole figures become, then, a necessity to distinguish between the two interpretations.

References

[1] T. Duangmanee, S. Wannakitti, R. Suwanwarangkul, S. Charojrochkul, Journal of Metals, Materials and Minerals 18 (2008) 7.

[2] J. W. Fergus, Journal of Power Sources 162 (2006) 30.

[3] K. Wada, N. Yamaguchi, H. Matsubara, Surf. Coat. Technol. 184 (2004) 55.

[4] N.P. Padture, M. Gell, E.H. Jordan, Science, vol.296, 5566 (2002) 280.

[5] P.K. Srivastava, T. Quach, Y.Y. Duan, R. Donelson, S.P. Jiang, F.T. Ciacchi, S.P.S. Badwal, Solid State Ionics 99 (1997) 311.

[6] J. Will, A. Mitterdorfer, C. Kleinlogel, D. Perednis, L.J. Gauckler, Solid State Ionics 131 (2000) 79.

[7] P. Gao, L.J. Meng, M.P. dos Santos, V. Teixeira, M. Andritschky, Thin Solid Films 377 (2000) 32.

[8] P. Briois, A. Billard, Surf. Coat. Technol. 201 (2006) 1328.

[9] V.V.Kharton, F.M.B. Marques, A. Atkinson, Solid State Ionics 174 (2004) 135.

[10] P. Holtappels, F.W. Poulsen, M. Mogensen, Solid State Ionics 135 (2000) 675.

[11]. B. Hobein, F. Tietz, D. Stöver, M. Cekada, P. Panjan, Journal of European Ceramic Society 21 (2001) 1843.

[12] H. Takebe H., D. Sakamoto D, O. Ohtaka, H. Fukui, A. Yoshiasa, T. Yamanaka, K. Ota, T. Kikegawa, J. Phys.: Condens. Matter 14 (2002) 11507.

[13] M. Backhaus-Ricoult, M. Badding, Y. Thibault, Ceramic transactions, 179 (2006) 173.

[14] C. Amaya, W. Aperador, J.C. Caicedo, F.J. Espinoza-Beltrán, J. Muñoz)Saldaña, G. Zambrano, P. Prieto, Corrosion Science 51 (2009) 2994.

[15] G. De Winter, S. Mahieu, I. De Roeck, R. De Gryse, J. Denul, IEEE Transactions on Applied Superconductivity, 13, 2 (2003) 2567.

[16] M. Saraiva, H. Chen, W. P. Leroy, S. Mahieu, N. Jehanathan, O. Lebedev, V. Georgieva, R. Persoons, D. Depla., Plasma Process. Polym., 6 (2009) S751.

[17] M. Saraiva, V. Georgieva, S. Mahieu, K. Van Aeken, A. Bogaerts, D. Depla, J. Appl. Phys., 107 (2010).

[18] S. Mahieu , P. Ghekiere, D. Depla, R. De Gryse Thin Solid Films 515 (2006) 1229–1249.

[19] J.S. Lamas, W.P.Leroy, D. Depla, Thin Solid Films (2011) doi: 10.1016/j.tsf.2011.10.179.

[20] M. Stahl, T. Trottenberg, H. Kersten Rev. Sci. Instrum. 81, (2010) 023504.

[21] S.D Ekpe, S. K. Dew, J. Vac. Sci. Technol., A 21 (2003) 476.

[22] Depla, D. & Mahieu, S. (2008). Reactive Sputter Deposition . Springer Series in Materials Science. Springer.

[23] G. M. Turner, J. Vac. Sci. Technol. A 13(4) (1995).

[24] J. A. Thornton, J. Vac. Sci. Technol. 15 (1978) 171.

[25] G. Buyle, W. De Bosscher, D. Depla, K. Eufinger, J. Haemers, R. De Gryse, Vacuum 70 (2003) 29.

[26] D. Depla, G. Buyle, J. Haemers, R. De Gryse, Surf. Coat. Technol. 200 (2006) 4329-4338.

[27] S.D. Ekpe, S.K. Dew, J. Vac. Sci. Technol., A 22 (2004) 1420.

[28] T.P. Drüsedau, T. Bock, T.M. John, F. Klabunde,W. Eckstein, J. Vac. Sci. Technol., A 17 (1999) 2896.

[29] S.D. Ekpe, S.K. Dew, J. Vac. Sci. Technol., A 20 (2002) 1877.

[30] S. Mahieu, D. Depla, J. Phys. D: Appl. Phys. 42 (2009): 16

[31] S. Mahieu , P. Ghekiere, D. Depla, R. De Gryse, O.I. Lebedev, G. Van Tendeloo, Journal of Crystal Growth 290 (2006) 272-279.

[32] S. Mahieu, W. P. Leroy, K. Van Aeken, and D. Depla, J. Phys. D: Appl. Phys. 106 (2009) 093302

[33] G. Z. Radnóczi, T. Seppänen, B. Pécz, L. Hultman, J. Birch, Phys. Stat. Sol. (a) 202, 7 (2005) R76–R78.

[34] M. Saraiva & D. Depla. (2012). Texture and microstructure in co-sputtered Mg-M-O (M=Mg, Al, Cr, Ti, Zr, and Y) films. Manuscript sumbitted for publication.

Figure captions

Fig.1 Polar plot graph comparing two different gas pressures.

Fig. 2 a) Thermal flux; b) Flux of metal particles; c) Energy per deposited atom vs. Y T-S distance at gas pressures of 0.5 and 0.95 Pa.

Fig. 3 SEM images on YSZ thin films; a) cross section view, Y T-S distance = 200 mm, p = 0.5 Pa, 25 at.% Y; b) surface image, Y T-S distance = 200 mm, p = 0.5 Pa; c) cross section view, Y T-S distance = 120 mm, p = 0.5 Pa, 40 at.% Y; d) cross section view, Y T-S distance = 220 mm, p = 0.95 Pa, 15 at.% Y.

Fig. 4. Representation of the calculated angle $\varphi = 12°$ and $\chi = 78°$ in a) a polar plot; b) stereographic projection and c) pole figure.

Fig. 5 Pole figures for YSZ films deposited at low pressure. Y T-S distance: a) 240 mm (8% Y); b) 200 mm (25% Y); c) 80 mm (60% Y). The first column indicates the [111] pole figure, the second the [200] pole figure and the third represents the schematic drawing of the cubic structure.

Fig. 6 Pole figures for YSZ films deposited at high pressure. Y T-S distance: a) 220 mm (15% Y); b) 140 mm (32% Y); c) 100 mm (46% Y). The first column indicates the [111] pole figure, the second the [200] pole figure and the third represents the schematic drawing of the cubic structure.

Fig.7a) Azimuthal and b) polar angle vs. composition showing the influence of the change of the substrate angle on the columnar tilt.

Fig.1

Click here to download high resolution image

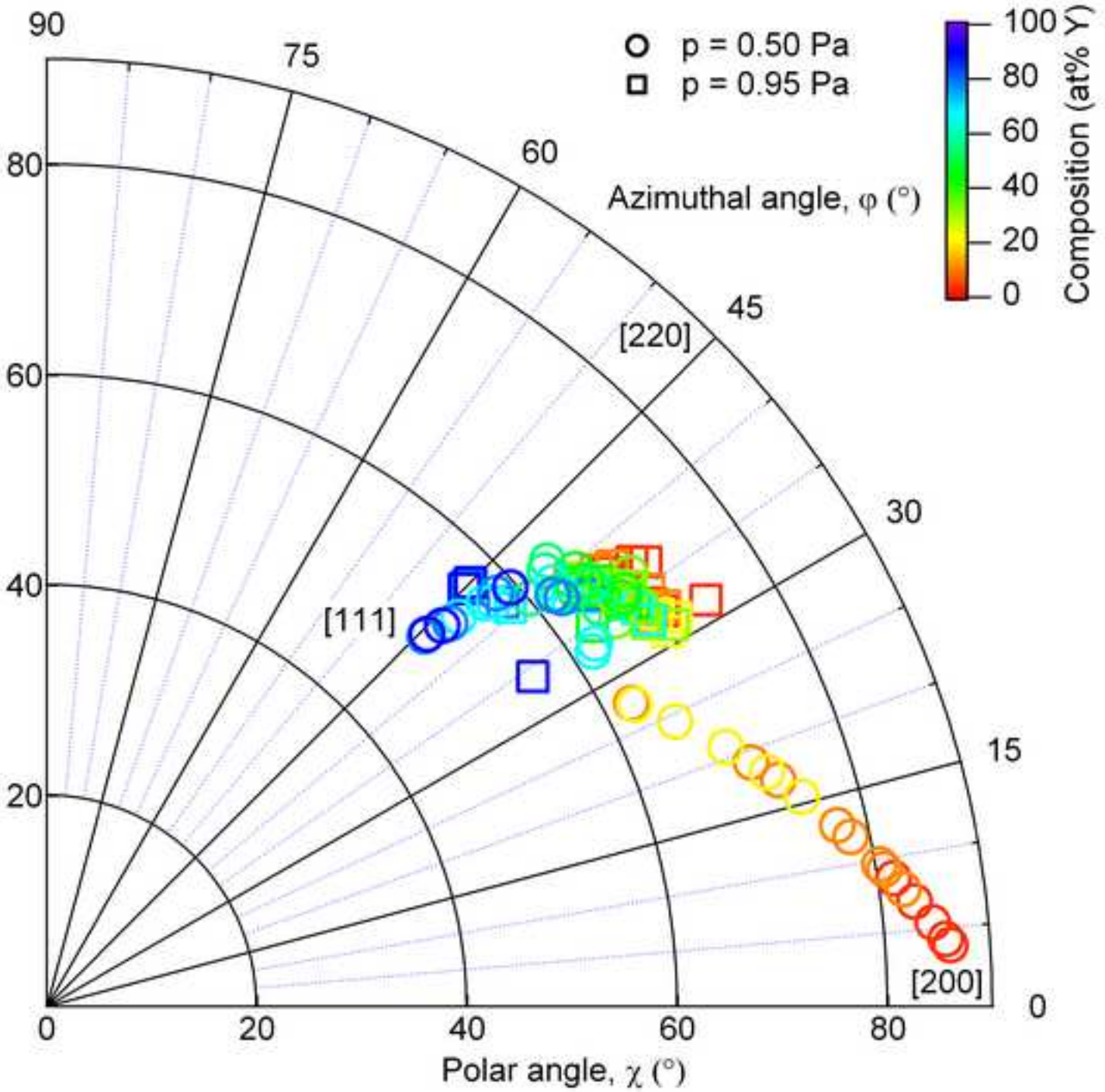

Fig.2

Click here to download high resolution image

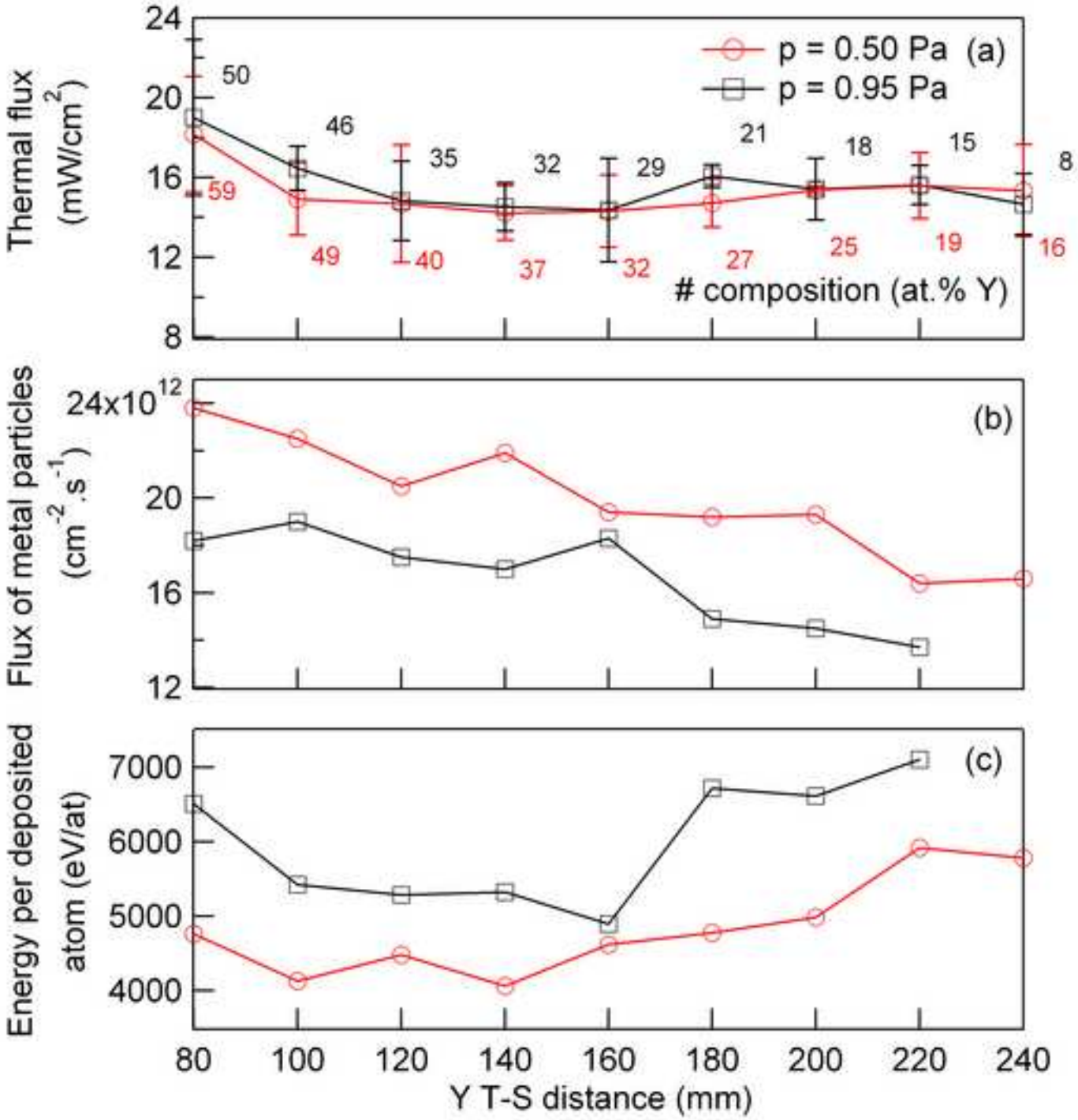

Fig.3a

Click here to download high resolution image

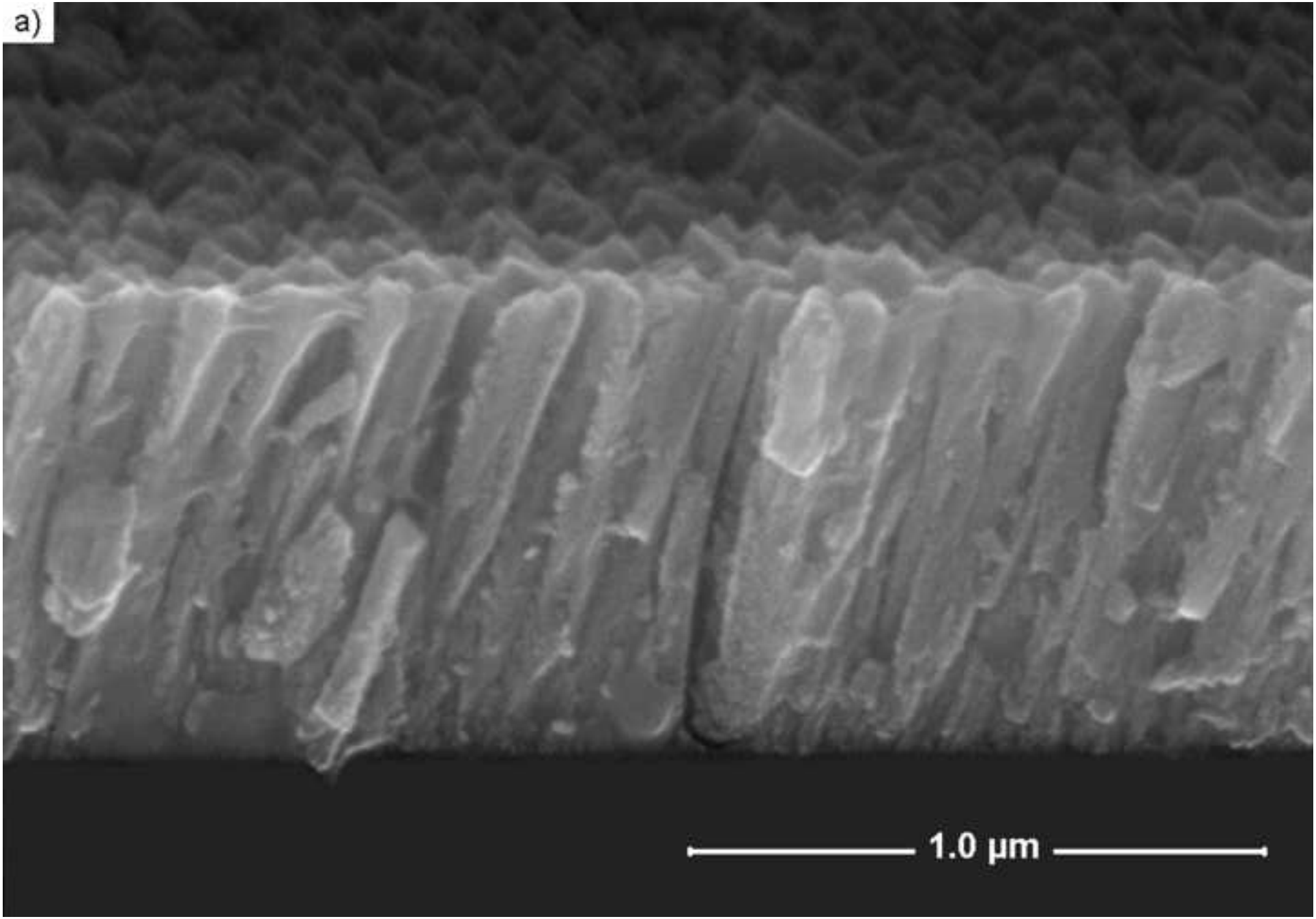

Fig.3b

Click here to download high resolution image

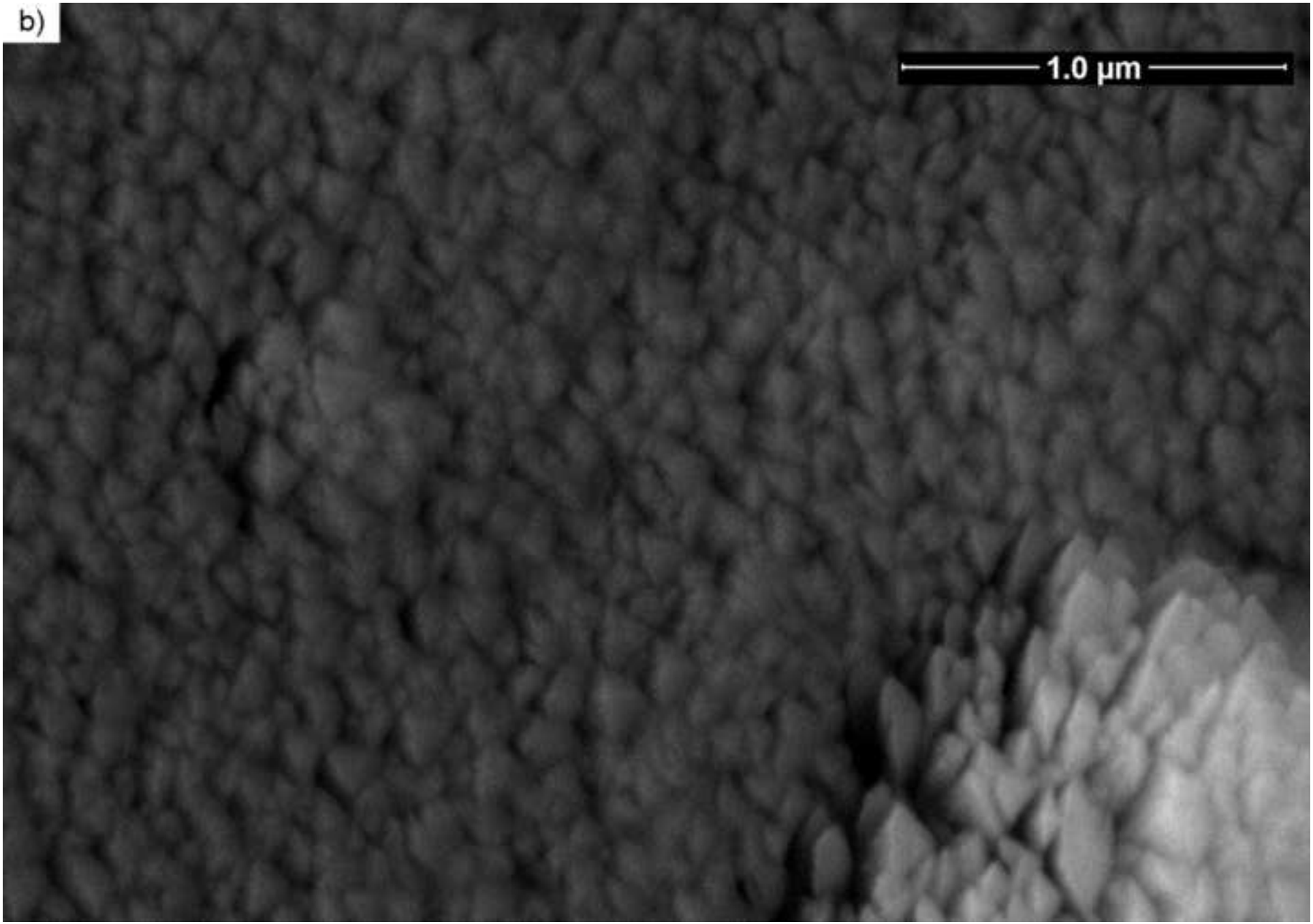

Fig.3c

Click here to download high resolution image

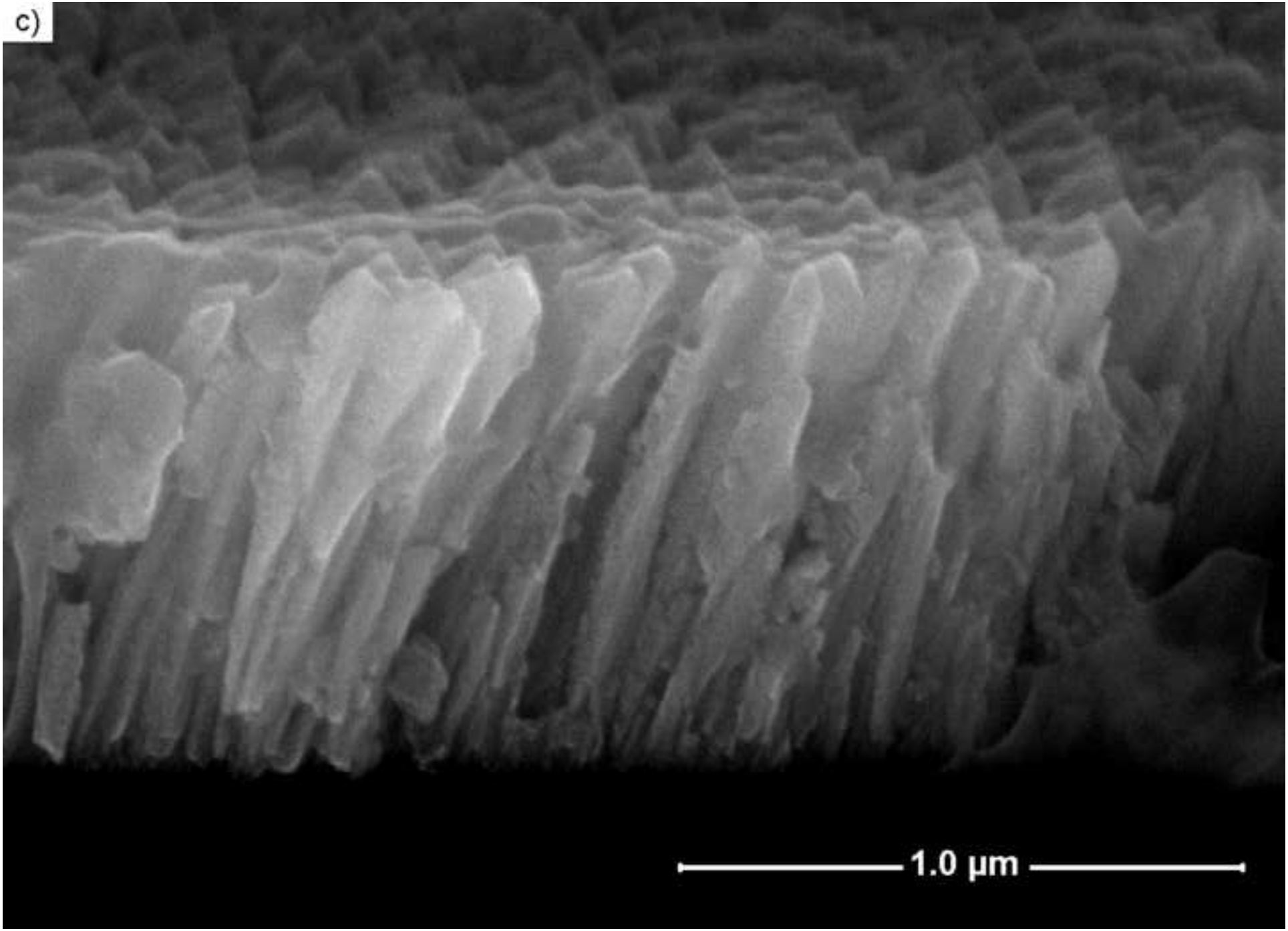

Fig.3d

Click here to download high resolution image

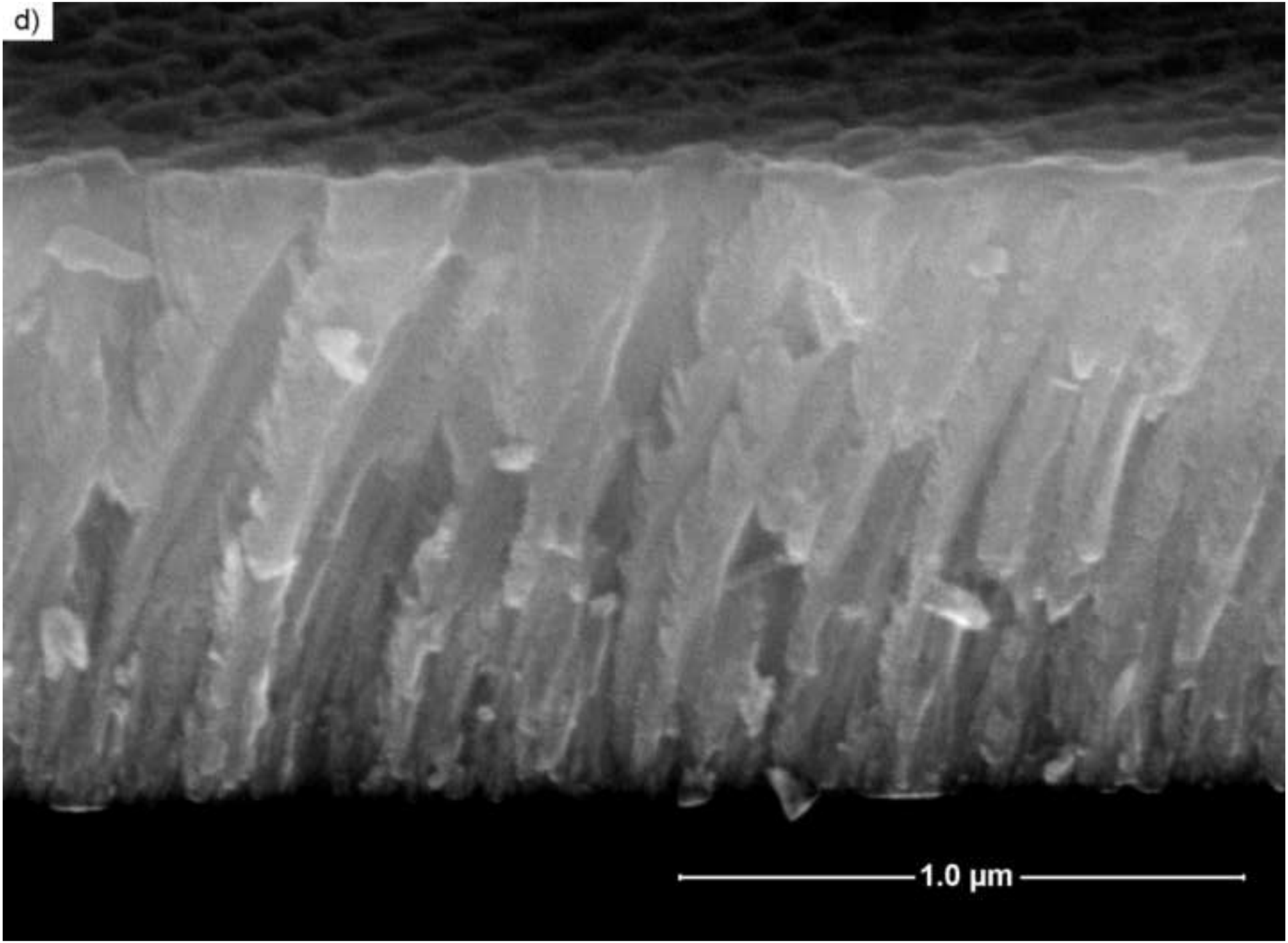

Fig.4

Click here to download high resolution image

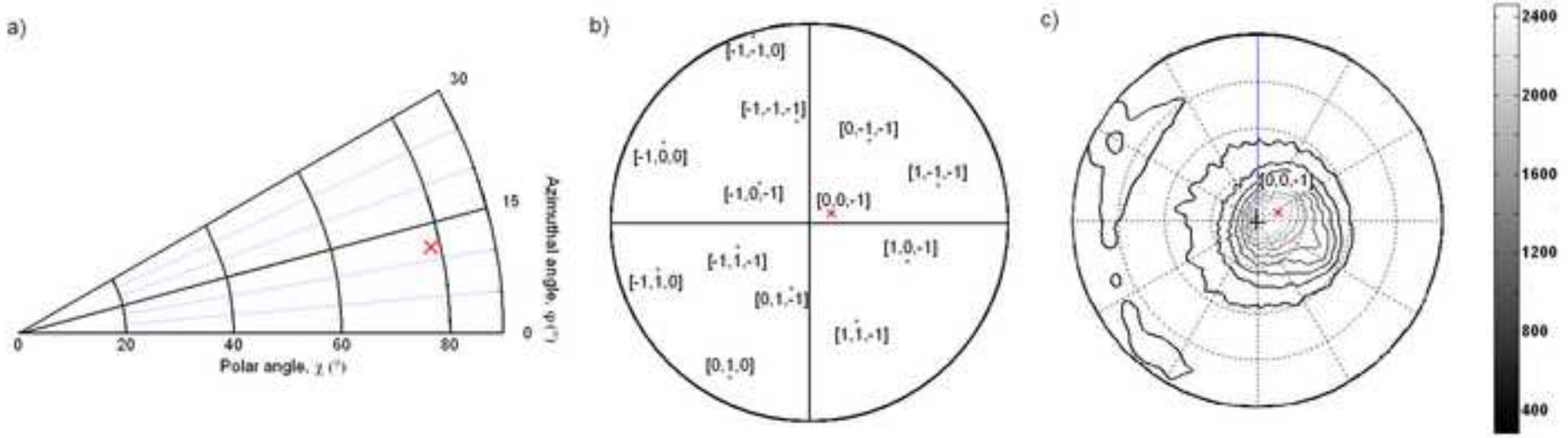

Fig.5a

Click here to download high resolution image

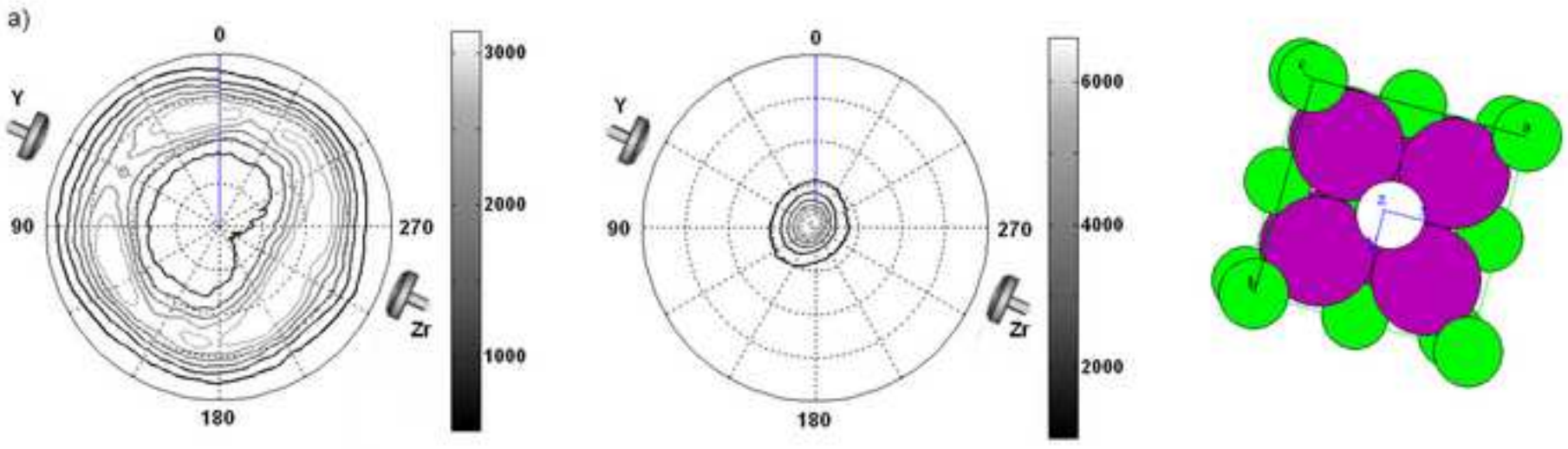

Fig.5b

Click here to download high resolution image

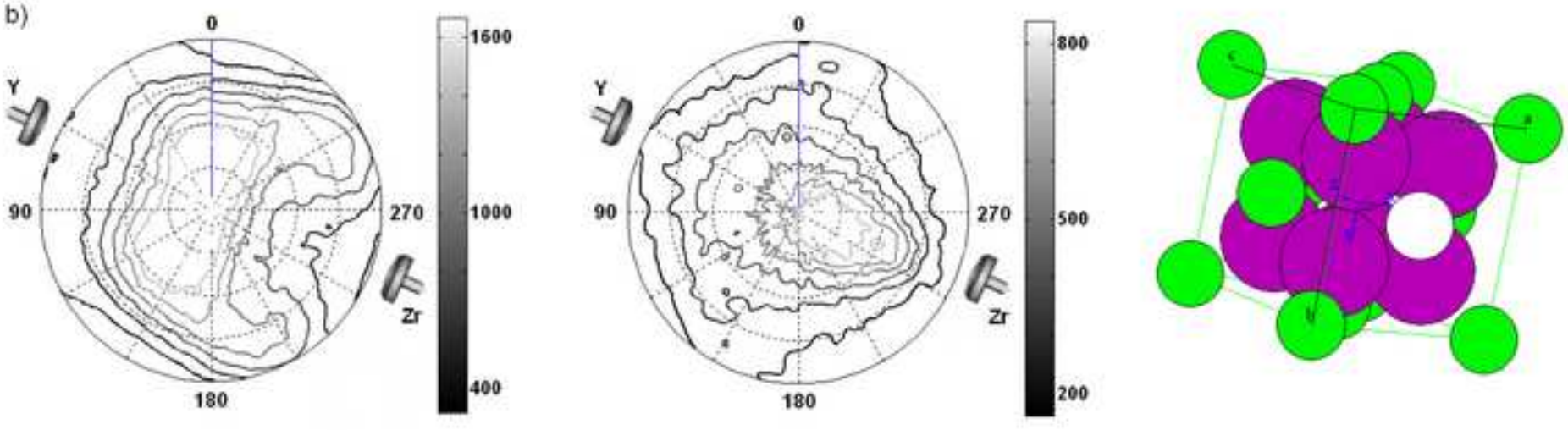

Fig.5c

Click here to download high resolution image

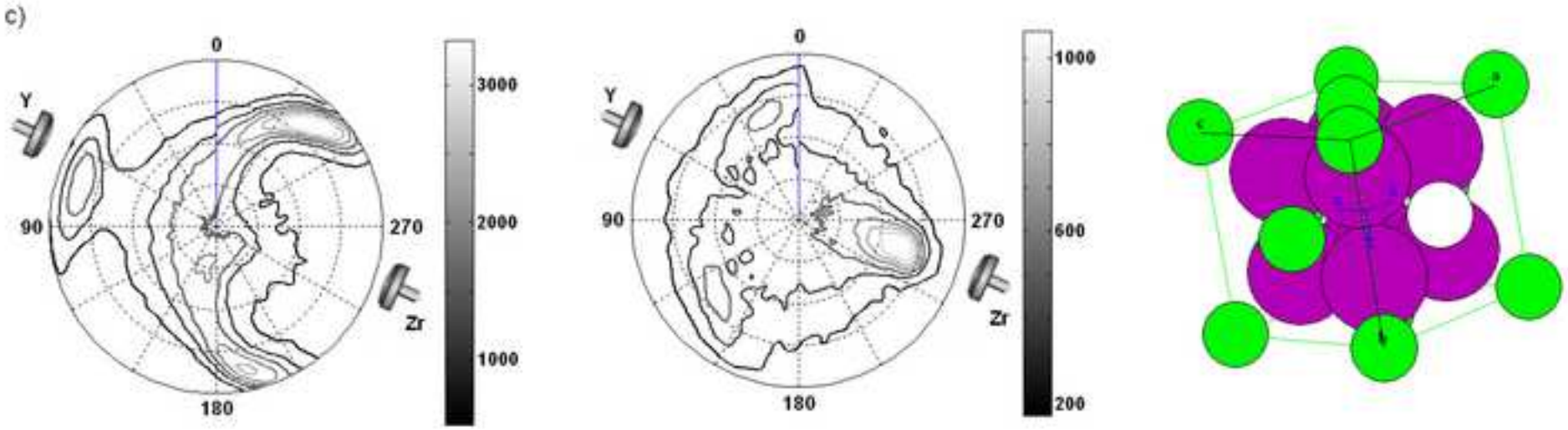

Fig.6a

Click here to download high resolution image

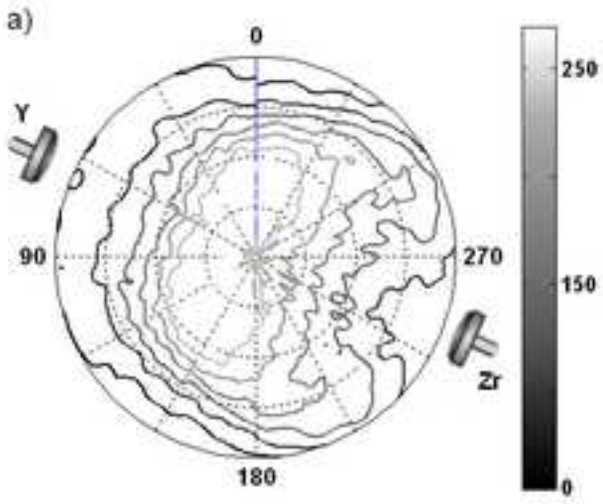

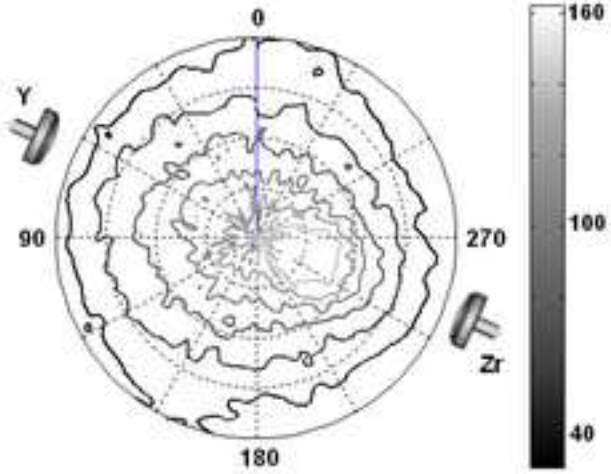

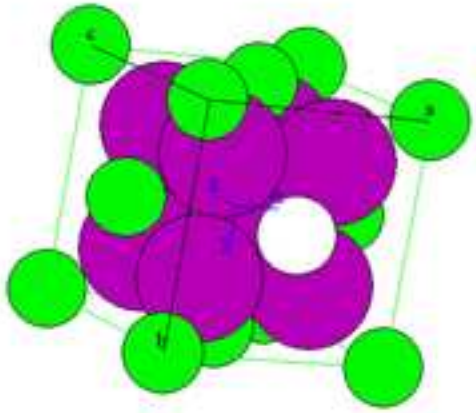

Fig.6b

Click here to download high resolution image

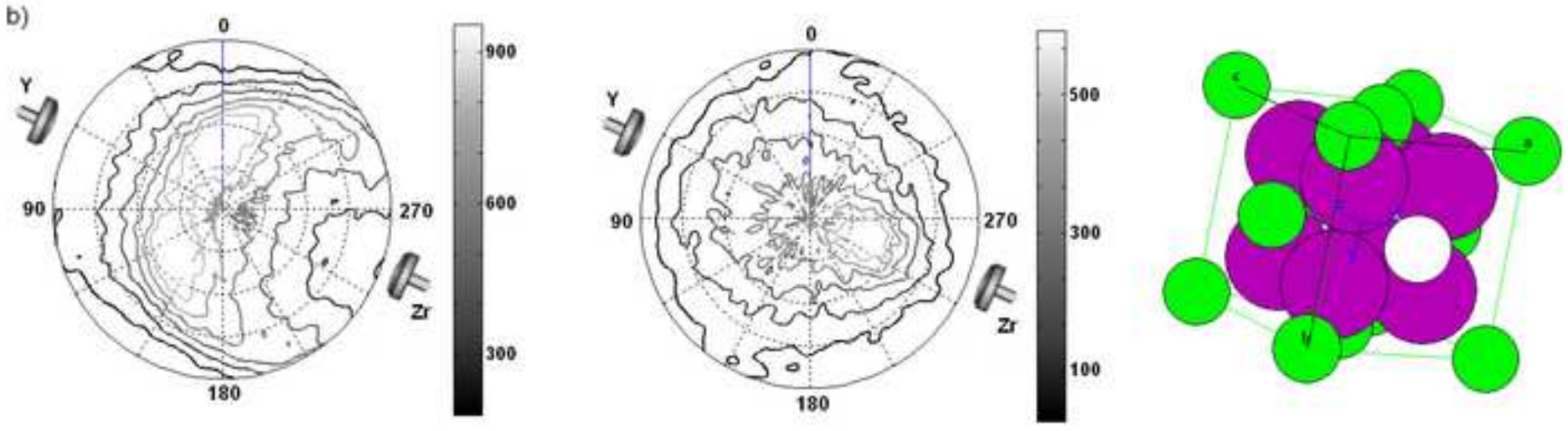

Fig.6c

Click here to download high resolution image

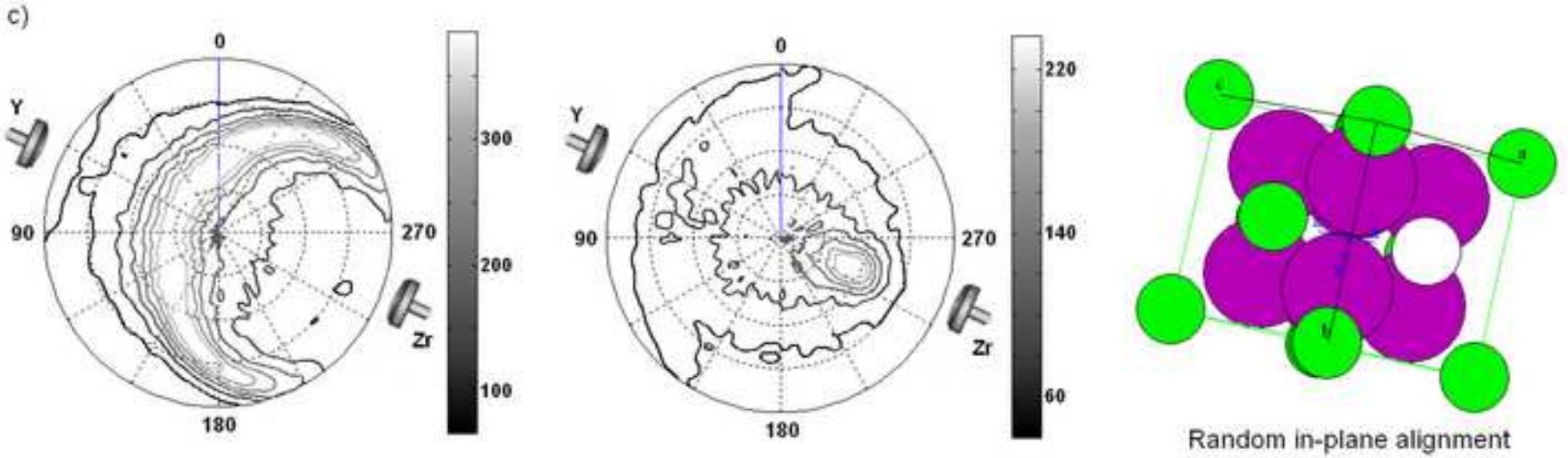

Fig.7a

Click here to download high resolution image

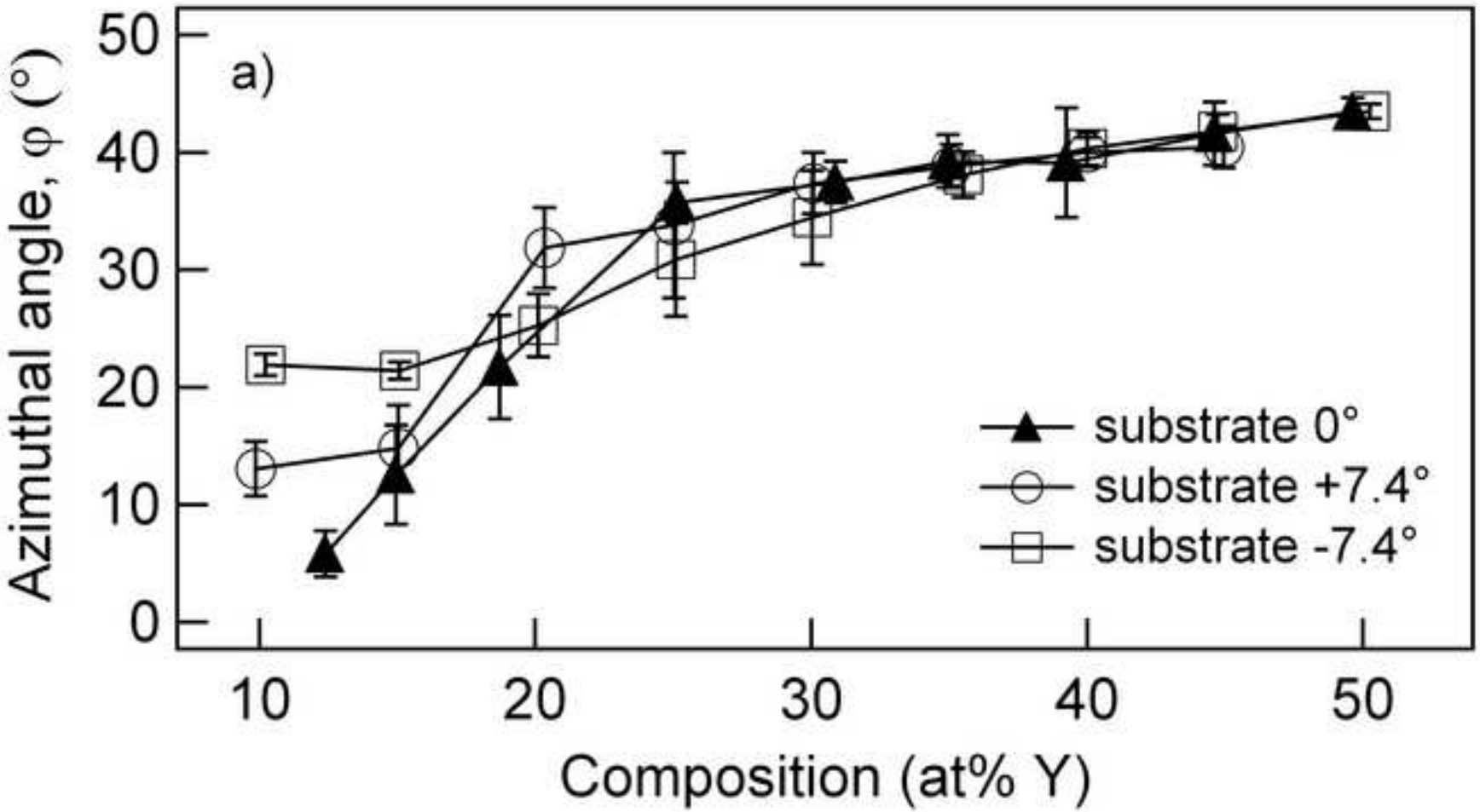

Fig.7b

Click here to download high resolution image